Published in final edited form as:
Immunity. 2011 December 23; 35(6): 986–996. doi:10.1016/j.immuni.2011.10.015.

Th17 Cells Induce Ectopic Lymphoid Follicles in Central Nervous System Tissue Inflammation

Anneli Peters[1], **Lisa A. Pitcher**[2], **Jenna M. Sullivan**[1], **Meike Mitsdoerffer**[1], **Sophie E. Acton**[3], **Bettina Franz**[3], **Kai Wucherpfennig**[3], **Shannon Turley**[3], **Michael C. Carroll**[2], **Raymond A. Sobel**[4], **Estelle Bettelli**[1,5,*], and **Vijay K. Kuchroo**[1,*]

[1]Center for Neurologic Diseases, Brigham and Women's Hospital, Harvard Medical School, Boston, MA 02115, USA

[2]The Immune Disease Institute and Program in Cellular and Molecular Medicine, Children's Hospital, Department of Pediatrics and Department of Pathology, Harvard Medical School, Boston, MA 02115, USA

[3]Department of Cancer Immunology and AIDS, Dana-Farber Cancer Institute, Boston, MA 02115, USA

[4]Palo Alto Veteran's Administration Health Care System and Department of Pathology, Stanford University School of Medicine, Stanford, CA 94305, USA

SUMMARY

Ectopic lymphoid follicles are hallmarks of chronic autoimmune inflammatory diseases such as multiple sclerosis (MS), rheumatoid arthritis, Sjögren's syndrome, and myasthenia gravis. However, the effector cells and mechanisms that induce their development are unknown. Here we showed that in experimental autoimmune encephalomyelitis (EAE), the animal model of MS, Th17 cells specifically induced ectopic lymphoid follicles in the central nervous system (CNS). Development of ectopic lymphoid follicles was partly dependent on the cytokine interleukin 17 (IL-17) and on the cell surface molecule Podoplanin (Pdp), which was expressed on Th17 cells, but not on other effector T cell subsets. Pdp was also crucial for the development of secondary lymphoid structures: Pdp-deficient mice lacked peripheral lymph nodes and had a defect in forming normal lymphoid follicles and germinal centers in spleen and lymph node remnants. Thus, Th17 cells are uniquely endowed to induce tissue inflammation, characterized by ectopic lymphoid follicles within the target organ.

INTRODUCTION

In multiple sclerosis (MS), lymphoid follicle-like structures are observed in close association with inflamed blood vessels in leptomeninges of patients with chronic progressive but not relapsing-remitting disease. These follicle-like structures appear to be in different stages of development, ranging from simple T and B cell clusters to well-organized follicles, encapsulated by reticulin lining, which contain T cells, proliferating B cells, plasma cells, and follicular dendritic cells, suggestive of germinal centers (GCs) (Magliozzi

*Correspondence: ebettelli@benaroyaresearch.org (E.B.), vkuchroo@rics.bwh.harvard.edu (V.K.K.).
[5]Present address: Benaroya Research Institute, Seattle, WA 98101, USA

SUPPLEMENTAL INFORMATION

Supplemental Information includes six figures and two tables and can be found with this article online at doi:10.1016/j.immuni.2011.10.015.

et al., 2007; Serafini et al., 2004). However, not all the features and definable markers of a secondary lymphoid follicle with discernable T and B cell zones and well-developed GCs are always observed in ectopic lymphoid follicle-like structures (eLFs) in the target organ in an autoimmune disease (Weyand et al., 2001). eLFs are able to drive chronic inflammation directly in the target organ, accelerate and/or maintain the disease process, and are often considered a hallmark of an aggressive chronic disease course (Weyand et al., 2001). We have previously shown that myelin oligodendrocyte glycoprotein (MOG)-specific 2D2 T cell receptor (TCR) transgenic T helper 1 (Th1) and Th17 cells can induce experimental autoimmune encephalomyelitis (EAE) with similar severity upon adoptive transfer into wild-type (WT) recipient mice (Jäger et al., 2009). Importantly, histological analysis of the central nervous system (CNS) revealed important differences between the CNS lesions of Th1 and Th17 cell recipients: the infiltrating cells in the CNS of Th17 cell recipients aggregated into relatively large organized structures reminiscent of eLFs, suggesting that Th17 cells may be able to induce eLF-like structures in the CNS. In this study, we show that Th17 cells are uniquely endowed to induce eLFs in the target tissue and that the signature cytokine interleukin 17 (IL-17) and the cell surface molecule Podoplanin (Pdp), which is expressed on Th17 cells, contribute to the development of eLFs.

RESULTS

Th17 Cell Recipients Form Ectopic Lymphoid Follicles in the CNS

After transfer of MOG-specific Th17 cells, CNS-infiltrating cells formed organized lymphoid aggregates in the subarachnoid space that were often located around or near blood vessels and surrounded by reticulin fibers (Figure 1A). Reticulin fibers are mainly composed of type III collagen, a structural molecule produced by stromal cells. In lymph nodes (LNs), collagen-positive fibers form networks and conduits that organize the follicles (Roozendaal et al., 2009). Immunohistochemical analysis revealed that the organized follicle-like structures in the CNS of Th17 cell recipients were composed of B cell clusters, surrounded by T cells and encapsulated by collagen fibers (Figures 1B and 1C). The fibers even extended into the center of B cell clusters, reminiscent of the collagen-lined conduits described in LN follicles (Roozendaal et al., 2009). Overall, the aggregates had variable degrees of organization and maturation; in some instances they markedly expanded the spinal cord subarachnoid space and extended over long areas in longitudinal sections (Figure 1C). Analysis of the infiltrates by flow cytometry confirmed the presence of both T and B cells in the CNS of Th17 cell recipients (Figure 2A). The majority of T cells (>80%) present in the CNS were transferred Th17 cells, as shown by the fact that they expressed the transgenic TCR chain Vα3.2 (Figure 2B). Notably, among both CNS-derived T and B cells, we detected expression of the GC marker GL7 (Figure 2C), as well as expression of another GC-marker PNA (Figure S1A available online), indicating that at least some of the CNS B and T cells exhibit features of cells undergoing a GC reaction in the eLF. Accordingly, 4%–7% of the CNS B cells were negative for IgD and IgM but positive for IgG and had thus undergone isotype switching (Figure S1B). In addition to regular B cells, we also found some $CD138^{+}CD11b^{-}$ plasma cells in the CNS (Figure S2A). T cells isolated from the CNS expressed CCR6, a chemokine receptor specifically expressed on Th17 cells, but we also observed expression of CXCR5, ICOS, and Bcl6 (Figure 2D). Because all of these molecules are expressed on follicular T helper (Tfh) cells, these data suggested that the transferred T cells may attain some features of Tfh cells in the CNS and provide help to the B cells. Interestingly, the $CXCR5^{+}$ T cells in the CNS were highly enriched for IL-17^{+} cells (Figure S1C). $CXCR5^{-}$ T cells in the CNS maintained a stable IL-17 phenotype (Figure S1C), similar to the Th17 cell cytokine profile before transfer (Figure S1D). In some but not all eLFs, we also detected the GC chemokine CXCL13 decorating the collagen lining within the CNS B cell clusters (Figure S2B). In addition to the protein expression, we also detected

significantly increased mRNA expression of CXCL13 in the spinal cords of sick Th17 cell recipients compared to spinal cords from equally sick MOG+CFA-immunized mice or healthy naive control mice (Figure S2C). These data indicate that Th17 cells promoted the expression of CXCL13 in the CNS, which may be responsible for organizing eLFs. Because follicular dendritic cells (FDCs) are a crucial component of LN follicles and GCs, we analyzed whether any FDCs were present in the eLFs. We indeed detected FDC-M1-positive cells in the CNS of Th17 cell recipients (Figure S3A). Of note, these cells differed from traditional FDCs in terms of their morphology and expression of CD11b and CD11c. Taken together, these data suggest that organized ectopic lymphoid follicles were formed in the CNS of Th17 cell recipients.

Th17 Cells, but Not Other Effector T Cell Subsets, Induce Formation of eLFs

Because Th17 cells induced eLF formation upon adoptive transfer, we wanted to determine whether other T cell subsets were also able to induce ectopic lymphoid structures. We compared the ability of various T cell subsets (Th1, Th2, Th9, and Th17), differentiated from naive MOG-specific 2D2 TCR transgenic T cells in vitro, to induce eLFs upon adoptive transfer. Only one of seven sick Th1 cell recipients and none of eight sick Th9 cell recipients formed eLFs in the CNS. Among Th2 cell recipients, only two of six mice developed mild EAE after transfer but did not have any eLFs. In contrast, about 73% of Th17 cell recipients (16 of 22) formed eLFs in the CNS with an average of 60 follicles per recipient (Figure 3A). Importantly, only Th17 cells exposed to IL-23, which maintain their IL-17-producing phenotype upon in vivo transfer (Jäger et al., 2009), induced the formation of eLFs. In contrast, Th17 cells differentiated in the presence of TGF-β plus IL-6 and low dose of IL-2, which do not maintain IL-17 production but convert to IFN-γ producers in vivo (Jäger et al., 2009), failed to induce eLF formation in recipient animals. These data indicate that Th17 cells, which stably produce Th17 cytokines, were especially equipped to induce the formation of eLFs, whereas other T cell subsets with the same antigen specificity, but different cytokine profile, did not induce eLF formation. We therefore wanted to determine which Th17-specific cytokines or surface molecules are responsible for Th17 cell-induced eLF formation.

Th17 cells produce a number of effector cytokines, including IL-17A, IL-17F, IL-21, and IL-22 (Bettelli et al., 2008), which could potentially contribute to disease induction and eLF formation. Among the Th17 effector cytokines, IL-17A and IL-21 have been shown to provide B cell help and induce antibody class switching (Doreau et al., 2009; King et al., 2008; Mitsdoerffer et al., 2010). To address the role of IL-17 in Th17 cell-induced EAE, we transferred Th17 cells into IL-17RA-deficient mice. Interestingly, IL-17RA-deficient mice developed attenuated EAE with significantly lower mean maximum disease score and delayed onset (Figure 3B; Table S1). In contrast to WT Th17 cell recipients, which often had atypical signs of EAE such as severe balance defects and weight loss, IL-17RA-deficient animals exhibited only classical signs of EAE. In line with the clinical data, histopathologic analysis revealed that IL-17RA-deficient mice had a slightly reduced number of CNS lesions and a slightly lower incidence of recipients developing eLFs in the CNS (55% [6 of 11] of *Il17ra*$^{-/-}$ recipients versus 73% of WT recipients) (Figure 3A, left). Importantly, there was also a reduction in the number of eLFs in the CNS of IL-17RA-deficient mice (28 ± 8 in *Il17ra*$^{-/-}$ recipients versus 60 ± 15 in WT recipients, $p = 0.0813$) (Figure 3A, right).

IL-21R-deficient recipients of Th17 cells developed slightly more severe EAE with higher incidence and mortality compared to the control group (Figure 3C; Table S1). Consistent with the clinical data, we observed a slight increase in the number of CNS lesions in *Il21r*$^{-/-}$ recipients and a slight increase in the percentage of recipients positive for eLFs (100%, 12 out of 12) (Figure 3A; Table S1). There was no significant difference in the number of eLFs

found in the CNS of IL-21R-deficient recipients (49 ± 9 in *Il21r*$^{-/-}$ versus 60 ± 15 in WT recipients, p = 0.5493) (Figure 3A).

Th17 Cells Express the Cell Surface Molecule Podoplanin

Aside from Th17 cell-specific effector cytokines, the unique ability of Th17 cells to form eLFs at specific anatomical sites may also depend on cell surface molecules preferentially expressed on Th17 cells. To find potential candidates, we performed gene expression profiling of T cells undergoing Th17 cell differentiation and identified two surface molecules, namely BLT1 and Podoplanin (Pdp, gp38), which were specifically expressed under Th17 cell-polarizing conditions (Figure S4A). We focused on the potential role of Pdp in forming eLFs. Pdp is a type I transmembrane sialomucin-like glycoprotein, which is expressed on different epithelia, including type I alveolar lining cells and lymphatic endothelium (Schacht et al., 2005); however, Pdp has not been reported to be expressed on T cells. The specific expression of Pdp and IL-17 on T cells under Th17 cell-polarizing conditions (IL-6 plus TGF-β or IL-21 plus TGF-β) was confirmed by quantitative PCR (Figure S4B). To test whether Pdp expression was restricted to Th17 cells, we differentiated sorted naive T cells into Th0, Th1, Th2, and Th17 cells in vitro and analyzed the different subsets for expression of Pdp (Figures 4A–4C). At the protein level, Pdp was expressed on 30%–70% of cells differentiated under Th17 cell-polarizing conditions, whereas Th0, Th1, and Th2 cell populations never expressed Pdp on more than 5% of differentiated cells (Figure 4A). Analysis of Th17 cells derived from IL-17-GFP reporter mice showed that the majority (>70%) of IL-17-GFP$^+$ T cells coexpressed Pdp (Figure 4B); however, 30% of T cells expressed Pdp without producing IL-17, indicating that Pdp expression does not always correlate with IL-17 production. Importantly, specific expression of Pdp on Th17 cells was maintained upon restimulation of the different T cell subsets, whereas restimulated Th1 and Th2 cells had only low or no detectable expression of Pdp-mRNA (Figure 4C). These data demonstrate that Pdp is stably expressed on Th17 cells only, not on other T helper cell subsets in vitro.

To determine whether Pdp is expressed on Th17 cells or other hematopoietic cells in vivo, we analyzed different cell types from LNs and spleen of naive IL-23R.GFP-KI mice for expression of Pdp by flow cytometry (Figure S4C). In IL-23R.GFP-KI mice, all of the IL-23R-expressing cells can be identified by GFP expression (Awasthi et al., 2009). Interestingly, almost all IL-23R.GFP$^+$CD11b$^+$CD11c^{int} antigen-presenting cells (APCs) and IL-23R.GFP$^+$CD4$^+$CD44$^+$ memory T cells also expressed Pdp on their surface. In addition, Pdp expression could be detected on 5%–12% of γδ T cells and all Pdp$^+$ γδ T cells were also IL-23R positive. Pdp was also detected on 10%–17% of NK cells in the LNs, whereas CD8$^+$ T cells and B cells were negative for Pdp. Importantly, the above-described expression pattern for Pdp was observed only in cells isolated from the LNs, not in splenocytes, which correlates with the differential IL-23R expression in these two compartments (Awasthi et al., 2009). Although Pdp expression was not directly regulated by IL-23R signaling (data not shown), it is possible that IL-23R and Pdp expression on hematopoietic cells are partly regulated by the same mechanisms, as indicated by the fact that the majority of IL-23R$^+$ cells was also positive for Pdp.

To investigate whether Pdp is expressed in vivo during the development of EAE, we first harvested LNs and spleen from IL-17-GFP reporter or WT mice on day 8 after immunization and analyzed the T cells for expression of IL-17-GFP and Pdp. Directly ex vivo, we found that T cells from lymph node and spleen expressed IL-17-GFP, but not Pdp (Figure S5A). However, after culturing the splenocytes with MOG for 4 days, we detected a small fraction of IL-17-GFP$^+$Pdp$^+$ T cells by flow cytometry (Figure 5A). These data indicate that in-vivo-generated Th17 cells upregulate Pdp only when they are exposed to antigen. To pursue this hypothesis further, we next isolated T cells from LNs, spleen, and

CNS at the peak of disease. Consistent with our previous observation, activated/memory T cells isolated from LNs or spleen did not express Pdp-mRNA, although they produced IL-17 (Figure 5B). In contrast, effector T cells isolated from the CNS expressed high levels of both Pdp- and IL-17-mRNA (Figure 5B). By using IL-17-GFP reporter mice undergoing EAE, we found that at the protein level, 80% of the IL-17-GFP$^+$ T cells isolated from the meninges coexpressed Pdp, whereas about 50% of the IL-17-GFP$^+$ cells isolated from the CNS parenchyma coexpressed Pdp (Figure 5C). However, there were also some IL-17-GFP$^+$ single-positive and Pdp$^+$ single-positive cells, consistent with the idea that not all IL-17 producers express Pdp and vice versa (Figure 4B). In general, the fraction of Pdp$^+$ cells was always higher in T cells isolated from the meninges compared to the parenchyma.

Because not only T cells but also APCs can express Pdp in vivo, we also analyzed Pdp expression on CD11b$^+$ cells during EAE. On day 8 after immunization, CD11b$^+$ cells in the LNs expressed Pdp similar to their naive counterparts (Figure S5C). About 1%–2% of the CD11b$^+$ cells in the spleen—which were completely negative for Pdp in the naive mouse—expressed Pdp on day 8 after immunization (Figure S5C). Analogous to the T cells, Pdp expression on CD11b$^+$ cells was increased during in vitro culture of splenocytes with MOG (Figure S5C). Next, both macrophages and microglia were isolated from the CNS and analyzed for Pdp-mRNA expression. CNS-infiltrating macrophages and, to a lesser extent, microglia expressed Pdp-mRNA during EAE (Figure S5B). At the protein level we found Pdp expression on both meningeal and parenchymal CD11b$^+$ APCs (Figure S5C).

Together, these data show that Pdp was highly expressed on proinflammatory cells including Th17 cells and CD11b$^+$ cells at the site of tissue inflammation and especially in the T cells that form infiltrates in the meninges.

Formation of eLFs Is Partly Dependent on Pdp

Because we observed the highest expression of Pdp on Th17 cells infiltrating the meninges during EAE, we wanted to determine whether Pdp plays a role in the formation of eLFs in Th17 cell recipients. In the CNS of Th17 cell recipients, we detected Pdp immunoreactivity around and within the eLFs, on T cells, macrophages, and collagen fibers (Figures S3B–S3D), indicating that Pdp is expressed on many essential components of the eLF. In addition, Pdp was constitutively expressed at high amounts in the meninges, which serve as an anchor point for eLFs. To determine whether Pdp is required for eLF formation, we treated Th17 cell recipients with a Pdp blocking antibody. Anti-Pdp-treated mice developed EAE with similar incidence and severity, but the onset was slightly delayed when compared to either PBS- or control-IgG-treated mice (Table S2; Figure 5D). However, histological analysis of the CNS revealed that anti-Pdp-treated mice had significantly reduced numbers of eLFs compared goat IgG/PBS-treated Th17 cell recipients (20 ± 2 versus 49 ± 12, $^*p = 0.0478$) (Figure 5D; Table S2), indicating that Pdp is very important for the formation of eLFs in the CNS of Th17 cell recipients.

Pdp Is Crucial for Formation of LNs and Secondary Lymphoid Structures

Because Pdp had a profound effect on the development of tertiary lymphoid structures in Th17 cell recipients, we wanted to determine whether Pdp also plays a role in the development of secondary lymphoid structures in vivo. Homozygous Pdp-deficient mice on the original 129-Sv background die within minutes after birth as a result of respiratory failure (Ramirez et al., 2003; Schacht et al., 2003). However, by crossing these mice with C57BL/6 mice, unexpectedly, some Pdp-deficient mice survived on the mixed background and reached adult age. Although all genotypes grossly appeared similar (Figure S6A), the peritoneal cavity and small intestine of Pdp-deficient mice was “bloody” (Figures S6B and S6C) and the Peyer’s patches (PP) were blood-filled and thus easily visible in Pdp-deficient

mice (Figure S6D). This is consistent with the proposed role of Pdp in the separation of blood and lymph vessels and thus, this “bloody” phenotype is caused by blood traveling through lymphoid vessels (Uhrin et al., 2010). Intriguingly, Pdp-deficient mice had another profound abnormality: they lacked macroscopically visible peripheral LNs (Figure S6E). Inguinal, brachial, axillary, and in most cases cervical LNs were absent in Pdp-deficient mice, and in their place were small blood-filled remnant structures (Figure S6F). Occasionally, Pdp-deficient mice possessed one normal-sized cervical and/or a mesenteric LN. These data indicate an important role for Pdp in the development of peripheral LNs. In contrast to the lack of LNs, Pdp-deficient mice had slightly enlarged spleens (Figure S6F). Formalin-fixed, paraffin-embedded sections of LN remnants and PP demonstrated that the structural organization with discernible lymphoid follicles and GCs normally observed in the WT was impaired in Pdp-deficient mice (Figure 6A); LN remnants contained only few lymphocytes mixed with extravasated blood cells. Similarly, the occasional cervical LN completely lacked organization and GC structures but was filled with homogeneous sheets of lymphocytes and hemosiderin, indicating prior extravasation of blood. PP of Pdp-deficient mice also seemed to have less conspicuous follicles compared to WT mice (Figure 6B). To test whether there is a defect in follicle formation in Pdp-deficient mice, we analyzed LN remnants and spleen of *Pdpn*$^{-/-}$ mice by confocal microscopy with GC-specific markers. LN remnants of Pdp-deficient mice contained unorganized T cells, few B cells, and hardly any GCs, which were identified by GL7-positive staining or by an FDC-specific stain (Figure 6C). Even in the spleens of Pdp-deficient animals, both size and number of GCs were dramatically reduced compared to WT littermates (Figure 6C). Within the PP, Pdp-deficient mice had significantly more underdeveloped/incomplete follicles containing very few or no FDCs compared to WT littermates (data not shown). These results suggest that Pdp-deficient mice have a major baseline defect in forming organized secondary lymphoid structures and generating follicles and GCs as observed in LNs, spleen, and PP.

DISCUSSION

Many human chronic autoimmune diseases are characterized by the presence of ectopic follicle-like structures in the target organ, and it has been suggested that eLFs exacerbate disease course and propagate chronic autoimmune inflammation (Weyand et al., 2001). We show here that Th17 cells induce formation of eLFs in the CNS during EAE. Although other T cell subsets with the same TCR specificity infiltrate both meninges and CNS parenchyma and induce clinical signs of EAE, they fail to induce formation of eLFs. Immunohistochemical characterization showed that the eLFs in the CNS of Th17 cell recipients displayed a wide range in their degree of maturation: although some merely constituted B cell aggregates, the majority of the B cell clusters were very structured and encapsulated by reticulin fibers. We found evidence that GC-like reactions are ongoing in some but not all of the eLFs, as suggested by the presence of CXCL13, PNA- and GL7-positive T and B cells, and plasma cells. In addition, we detected expression of the Tfh cell-associated molecules CXCR5, ICOS, and Bcl6 on the CNS T cells, indicating that the transferred Th17 cells may fulfill tasks of Tfh cells that are essential for the GC reaction (Mitsdoerffer et al., 2010). In support of this hypothesis, IL-21R-deficient recipients of Th17 cells also developed eLFs in the CNS despite their lack of endogenous Tfh cells, which require IL-21 as an autocrine growth and differentiating factor (Vogelzang et al., 2008). Our transfer experiments with IL-21R-deficient recipients suggest that IL-21R signaling in host cells (but not transferred Th17 cells) may be dispensable for disease induction and eLF formation by Th17 cells. Because IL-21 is known to promote B cell differentiation and isotype switching (Spolski and Leonard, 2008), this result was surprising. However, besides acting as an amplification factor for Th17 and Tfh cells (Vogelzang et al., 2008; Korn et al., 2007), IL-21 also induces IL-10-producing Tr1 cells (Pot et al., 2009), which are known to

limit tissue inflammation in autoimmune diseases (Fitzgerald et al., 2007). Therefore, the increased disease severity in IL-21R-deficient mice may be due to a defect in generating regulatory Tr1 cells and thus controlling Th17 cell-induced tissue inflammation.

Our transfer experiments with IL-17RA-deficient recipients showed that IL-17 contributes to disease severity and may be responsible for the development of atypical signs of EAE. Previous studies have associated atypical signs of EAE with lesions in the brainstem and cerebellum, which appear to be especially sensitive to IL-17-mediated inflammation but protected by the Th1 cytokine IFN-γ (Lees et al., 2008; Stromnes et al., 2008). Notably, our data also suggest that IL-17 itself may contribute to eLF formation, which is consistent with a recent report showing that IL-17 and Th17 cells promote the spontaneous formation of GCs in the spleen of autoimmune-prone BXD2 mice (Hsu et al., 2008).

Aside from specific cytokines like IL-17, Th17 cells may also rely on specialized surface molecules to promote eLF formation, which could explain why eLFs always appear at defined anatomical sites. Podoplanin is specifically expressed on Th17 cells in vitro, but in-vivo-generated Th17 cells express Pdp only upon reactivation with antigen in a recall assay or once they enter the CNS, suggesting that Pdp is important for Th17 effector cell functions in the target organ. Pdp appears to play an important role in the process of eLF formation, because blocking of Pdp in vivo significantly reduced the number of eLFs in the CNS of Th17 cell recipients. It is possible that—owing to their expression of Pdp—Th17 cells can attach themselves better to the meninges than other T cell subsets and thus promote eLF formation in the subarachnoid space. Whether the blocking of Pdp on Th17 cells themselves or on other cell types (macrophages, stromal, and parenchymal cells) leads to the reduction in eLFs in vivo remains to be determined. Nevertheless, our data underscore the role of Pdp in forming eLFs during an autoimmune reaction. Notably, Pdp expression on parenchymal tissue and macrophages was observed not only in Th17 cell recipients, but also in Th1 cell recipients (data not shown), suggesting that expression of Pdp on stromal or tissue cells and macrophages alone may not be sufficient for the formation of eLFs in the CNS.

It is interesting that the reduction of eLFs observed in anti-Pdp-treated Th17 cell recipients did not result in diminution of clinical disease, which may lead to the conclusion that eLFs do not contribute to clinical disease in EAE, contrary to a previous report (Columba-Cabezas et al., 2006). However, it is more likely that the clinical effects of eLF formation cannot be observed in such a short acute disease model, in which the clinical signs are also due to other pathological processes, including edema, inflammation, and demyelination in the CNS. Clinical effects of eLFs might be more apparent in a chronic disease model that resembles chronic progressive disease in MS—in which eLFs are most often observed (Magliozzi et al., 2007; Serafini et al., 2004).

The defects we described in the development of secondary lymphoid structures of Pdp-deficient mice further emphasize the importance of Pdp for the proper organization and formation of lymphoid structures. However, we want to point out that the observed defects in the development of secondary lymphoid organs are due not simply to Pdp-deficient T cells, but also to impaired development and/or function of several different cell types including FDCs and stromal cells—especially fibroblastic reticular cells (FRCs) and lymphoid endothelial cells—which all express Pdp (Hirakawa et al., 2003; Schacht et al., 2005). In addition, it has been shown that Pdp deficiency leads to formation of inadequately functioning lymphatic vessels (Schacht et al., 2003; Uhrin et al., 2010), which may also contribute to the observed defects within the secondary lymphoid structures. The mechanism by which Pdp promotes formation of lymphoid structures is not clear. CLEC-2, a C-type lectin-like receptor expressed on platelets (Suzuki-Inoue et al., 2006), neutrophils (Kerrigan et al., 2009), and DCs (Colonna et al., 2000), has been identified as a ligand for Pdp

(Suzuki-Inoue et al., 2007). Thus, formation of secondary and tertiary lymphoid structures might be enhanced by interaction of Pdp on stromal cells and T cells with CLEC-2 on DCs.

Taken together, we propose that the specific expression of Pdp on Th17 cells together with the presence of Th17-specific cytokines like IL-17 may act in concert to promote the formation of eLFs in the CNS. Because Pdp is crucial during development for the formation of LNs and other secondary lymphoid structures, it is tempting to speculate that Pdp is coopted by Th17 cells to form tertiary lymphoid structures in the target tissues during autoimmune inflammation. Therefore, IL-17 and Pdp may provide important targets in regulating tissue inflammation where ectopic lymphoid follicles play an important role in propagation of autoimmune diseases.

EXPERIMENTAL PROCEDURES

Animals

2D2 mice (Bettelli et al., 2003) and IL-23R.GFP-KI mice (Awasthi et al., 2009) were described previously. *Il21r*$^{-/-}$ mice (Kasaian et al., 2002) were provided by M. Grusby (Harvard School of Public Health, Boston, MA), *Il17ra*$^{-/-}$ mice (Ye et al., 2001) by J. Kolls (LSU Health Science Center, New Orleans, LA), and *Pdpn*$^{-/-}$ mice on 129Sv background (Ramirez et al., 2003) by M. Ramirez (Boston University, Boston, MA). IL-17A-GFP reporter mice were generated and provided by Y. Shen (Biocytogen, Worcester, MA). Mice were housed in a specific-pathogen-free, viral-antibody-free animal facility at the Harvard Institutes of Medicine. All breeding and experiments were reviewed and approved by the Institutional Animal Care and Use Committee of Harvard Medical School.

Induction and Assessment of EAE

Differentiation of naive MOG-specific T cells into different subsets followed by adoptive transfer into C57BL/6 recipient mice for the induction of EAE was performed as described previously (Jäger et al., 2009; see also http://kuchroo-lab.bwh.harvard.edu/KuchrooFrequentlyRequestedProtocols.htm). In brief, sorted naive T cells from 2D2 mice were differentiated into different T cell subsets in vitro and tested for cytokine production after 4 days. After 6–7 days, cells were restimulated in vitro with CD3 and CD28 antibodies for 48 hr. 2.5–3 × 10^6 cytokine-producing cells were injected intravenously into C57BL/6 recipients. For antibody treatment of Th17 cell recipients, mice were injected intravenously with 100 μg polyclonal anti-murine Podoplanin antibody or 100 μg Normal Goat IgG (R&D Systems, Minneapolis, MN) or PBS on day 0, 2, 4, and 7 after Th17 cell transfer.

Induction of EAE by immunization with MOG in CFA, recall assays, and isolation of cells from the CNS were performed as described previously (Awasthi et al., 2009; Jäger et al., 2009).

Animals were monitored daily for the development of classical and atypical signs of EAE according to the following criteria: 0, no disease; 1, decreased tail tone or mild balance defects; 2, hind limb weakness, partial paralysis, or severe balance defects that cause spontaneous falling over; 3, complete hind limb paralysis or very severe balance defects that prevent walking; 4, front and hind limb paralysis or inability to move body weight into a different position; 5, moribund state.

Histology and Immunohistochemistry

CNS, LNs, spleen, and PP were formalin fixed and paraffin embedded and slides were analyzed after Luxol fast blue-hematoxylin and eosin stains, silver stain, or incubation with

Podoplanin antibody (8.1.1)/Syrian Hamster IgG isotype control (SHG-1) (BioLegend). For immunohistochemistry of LNs, LN remnants, spleen, and PP were snap-frozen in OCT medium and cut in 8 μm sections. For immunohistochemistry of the CNS, mice were perfused 30–40 days after Th17 cell transfer with 4% paraformaldehyde. CNS was dehydrated in 30% sucrose for 24 hr and frozen in OCT medium. 8 μm sections were fixed in acetone, incubated with anti-FcR (2.4G2), and stained with the following antibodies in PBS containing 1% bovine serum albumin and 0.1% saponin for collagen stainings: αCD4-FITC and APC (RM4-5), αPdp-A488 and biotinylated (8.1.1), syrian hamster IgG isotype control (SHG-1), αCD11b-APC and PE (M1/70), Armenian hamster αCD11c (N418), αB220-APC (RA3-6B2) (all from BioLegend); rabbit α-typeI-collagen (Rockland Immunochemicals); biotinylated αB220 (RA3-6B2), Armenian hamster αCD3 (145-2C11), αCD35-A488 (8C12), FDC-M1-A488, (all produced and labeled in house); αCD138-PE or biotinylated (281-2), GL7-FITC, Streptavidin-PE (all from BD PharMingen); biotinylated αCXCL13, (from R&D Systems); Streptavidin-A633 and A488, α-rabbit-A568 and A633, goat α-rat-A488 (all from Invitrogen); α-Armenian hamster-DyLight488 and Cy3 (Jackson ImmunoResearch). Images were acquired on a Zeiss-BioRad Radiance 2000 MP confocal microscope.

Quantification of Lymphoid Aggregates

Lymphoid follicle-like aggregates were counted in Luxol fast blue-H&E-stained paraffin sections of the entire CNS of each mouse by a neuropathologist who was blinded to the clinical, genotype, and treatment parameters. Each sample counted contained representative 8 μm thick sections of 5 levels of brain tissue and 15–20 sections of spinal cord tissue. Thus, both the sampling and total areas of CNS tissue analyzed were uniform for each mouse. Leptomeningeal lymphoid infiltrates were frequently confluent but were counted as individual lymphoid follicles when there were round or ovoid aggregates with at least five mononuclear cell layers. Some aggregates showed central GCs in the routine sections, but most aggregates were small and round (i.e., mature-appearing lymphoid cells).

Flow Cytometry

The following antibodies were used for flow cytometry: αCD4-PerCP or PE or PECy7 or Pacific Blue (RM4-5), αCD62L-PE (MEL-14), αCD44-PE (IM7), αIFN-γ-PE (XMG1.2), αIL-17-APC or PE (TC11-18H10.1), αIL-10-PE (JES5-10E3), αCD11b-Pacific Blue or APC (M1/70), αCD11c-PE or PECy7 (N418), αCD19-APCCy7 or PE or PECy7 (6D5), αICOS-PE or PECy7 (7E.17G9), αNK1.1-APC (PK136), α-mo use IgD-PE (11-26C.2a), αPdp-FITC or biotinylated (8.1.1), and the corresponding isotype control Syrian hamster IgG (SHG-1), rat IgG2a-PE or APC isotype control (RTK2758), mouse IgG1-PE isotype control (MOPC-21), Armenian hamster IgG-PE or PECy7 isotype control (HTK888), and Streptavidin-APC were all purchased from BioLegend. αCD8-PECy7 (53-6.7), αIL-17F-A647 (eBio18F10), and α-γδ-TCR-PE (eBioGL3) were purchased from eBioscience (San Diego, CA, USA). αVα3.2 TCR-biotin or FITC (RR3-16), αCD3-APC-Cy7 (1452C11), GL7-FITC, αCXCR5-PE (2G8), αCCR6-A647 (140706), αCD138-APC (281-2), α-mouse IgM-biotin (II/41), α-mouse IgG1-PE (A85-1), rat IgM-FITC isotype control (R4-22), and αBcl6-PE (K112-91) were all purchased from BD PharMingen (San Diego, CA, USA). α-mouse IgG2a-PE (SB84A), α-mouse IgG2b-PE, and α-mouse IgG3-PE (LO-MG3) were purchased from Southern Biotech (Birmingham, AL, USA). Biotinylated α-PNA was purchased from Vector Laboratories (Burlingame, CA, USA).

All flow cytometry data were acquired on a BD FACSCalibur or BD LSRII and analyzed with FlowJo Tree Star software.

Quantitative PCR

RNA was extracted from cells with the RNeasy Kit (QIAGEN) according to the manufacturer's instructions. For extraction of total RNA from the spinal cord, mice were perfused with PBS and spinal cords were homogenized in TRIzol Reagent (Ambion). RNA was isolated according to the manufacturer's instructions, treated with the RNase-Free DNase Set (QIAGEN) to remove low-level DNA contamination, and purified via the RNA Cleanup protocol (QIAGEN). 1–2 μg RNA was then transcribed into cDNA with the iScript cDNA Synthesis Kit (BIO-RAD) according to the manufacturer's instructions. Quantitative PCR primers and probes were purchased from Applied Biosystems (IL-17A, Mm00439619_m1; Pdp, Mm00494716_m1; CXCL13, Mm00444534_m1; β-Actin, 4352341E).

Statistics

All error bars shown represent SEM. For the quantification of eLFs shown in Figures 3A (right) and 5D (right), only mice with ten or more eLFs were included in the analysis. Whether differences between groups are significant was determined with an unpaired Student's t test with a Welch's correction because the variances within the groups were significantly different. In Figures 3B and 3C, a linear regression analysis was performed to determine whether the differences between the groups are significant. All other data including data shown in Tables S1 and S2, Figure S2C, and Figure 5D (left) were tested for significant differences by an unpaired Student's t test.

Supplementary Material

Refer to Web version on PubMed Central for supplementary material.

Acknowledgments

We thank M. Ramirez (Boston University, Boston, MA) for generously sharing *Pdpn*$^{-/-}$ mice with us. We thank D. Kozoriz for cell sorting. A.P. is a graduate student jointly supervised by R. Heumann (Ruhr-University Bochum, Germany) and V.K.K. This work was supported by grants from the NIH (1R01NS059996 to E.B., 5T32HL066987-09 to L.A.P., and R01NS045937, R01NS035685, R37NS030843, R01A1044880, P01A1039671, P01NS038037, and a Javits Neuroscience Investigator Award to V.K.K.) and the National Multiple Sclerosis Society (NMSS Transition Award TA3014A1/1 to E.B. and RG-2571 to V.K.K.). A.P. is the recipient of a Ph.D. scholarship by the Boehringer Ingelheim Fonds.

References

Awasthi A, Riol-Blanco L, Jäger A, Korn T, Pot C, Galileos G, Bettelli E, Kuchroo VK, Oukka M. Cutting edge: IL-23 receptor gfp reporter mice reveal distinct populations of IL-17-producing cells. J Immunol. 2009; 182:5904–5908. [PubMed: 19414740]

Bettelli E, Pagany M, Weiner HL, Linington C, Sobel RA, Kuchroo VK. Myelin oligodendrocyte glycoprotein-specific T cell receptor transgenic mice develop spontaneous autoimmune optic neuritis. J Exp Med. 2003; 197:1073–1081. [PubMed: 12732654]

Bettelli E, Korn T, Oukka M, Kuchroo VK. Induction and effector functions of T(H)17 cells. Nature. 2008; 453:1051–1057. [PubMed: 18563156]

Colonna M, Samaridis J, Angman L. Molecular characterization of two novel C-type lectin-like receptors, one of which is selectively expressed in human dendritic cells. Eur J Immunol. 2000; 30:697–704. [PubMed: 10671229]

Columba-Cabezas S, Griguoli M, Rosicarelli B, Magliozzi R, Ria F, Serafini B, Aloisi F. Suppression of established experimental autoimmune encephalomyelitis and formation of meningeal lymphoid follicles by lymphotoxin beta receptor-Ig fusion protein. J Neuroimmunol. 2006; 179:76–86. [PubMed: 16870269]

Doreau A, Belot A, Bastid J, Riche B, Trescol-Biemont MC, Ranchin B, Fabien N, Cochat P, Pouteil-Noble C, Trolliet P, et al. Interleukin 17 acts in synergy with B cell-activating factor to influence B cell biology and the pathophysiology of systemic lupus erythematosus. Nat Immunol. 2009; 10:778–785. [PubMed: 19483719]

Fitzgerald DC, Zhang GX, El-Behi M, Fonseca-Kelly Z, Li H, Yu S, Saris CJ, Gran B, Ciric B, Rostami A. Suppression of autoimmune inflammation of the central nervous system by interleukin 10 secreted by interleukin 27-stimulated T cells. Nat Immunol. 2007; 8:1372–1379. [PubMed: 17994023]

Hirakawa S, Hong YK, Harvey N, Schacht V, Matsuda K, Libermann T, Detmar M. Identification of vascular lineage-specific genes by transcriptional profiling of isolated blood vascular and lymphatic endothelial cells. Am J Pathol. 2003; 162:575–586. [PubMed: 12547715]

Hsu HC, Yang P, Wang J, Wu Q, Myers R, Chen J, Yi J, Guentert T, Tousson A, Stanus AL, et al. Interleukin 17-producing T helper cells and interleukin 17 orchestrate autoreactive germinal center development in autoimmune BXD2 mice. Nat Immunol. 2008; 9:166–175. [PubMed: 18157131]

Jäger A, Dardalhon V, Sobel RA, Bettelli E, Kuchroo VK. Th1, Th17, and Th9 effector cells induce experimental autoimmune encephalomyelitis with different pathological phenotypes. J Immunol. 2009; 183:7169–7177. [PubMed: 19890056]

Kasaian MT, Whitters MJ, Carter LL, Lowe LD, Jussif JM, Deng B, Johnson KA, Witek JS, Senices M, Konz RF, et al. IL-21 limits NK cell responses and promotes antigen-specific T cell activation: a mediator of the transition from innate to adaptive immunity. Immunity. 2002; 16:559–569. [PubMed: 11970879]

Kerrigan AM, Dennehy KM, Mourão-Sá D, Faro-Trindade I, Willment JA, Taylor PR, Eble JA, Reis e Sousa C, Brown GD. CLEC-2 is a phagocytic activation receptor expressed on murine peripheral blood neutrophils. J Immunol. 2009; 182:4150–4157. [PubMed: 19299712]

King C, Tangye SG, Mackay CR. T follicular helper (TFH) cells in normal and dysregulated immune responses. Annu Rev Immunol. 2008; 26:741–766. [PubMed: 18173374]

Korn T, Bettelli E, Gao W, Awasthi A, Jäger A, Strom TB, Oukka M, Kuchroo VK. IL-21 initiates an alternative pathway to induce proinflammatory T(H)17 cells. Nature. 2007; 448:484–487. [PubMed: 17581588]

Lees JR, Golumbek PT, Sim J, Dorsey D, Russell JH. Regional CNS responses to IFN-gamma determine lesion localization patterns during EAE pathogenesis. J Exp Med. 2008; 205:2633–2642. [PubMed: 18852291]

Magliozzi R, Howell O, Vora A, Serafini B, Nicholas R, Puopolo M, Reynolds R, Aloisi F. Meningeal B-cell follicles in secondary progressive multiple sclerosis associate with early onset of disease and severe cortical pathology. Brain. 2007; 130:1089–1104. [PubMed: 17438020]

Mitsdoerffer M, Lee Y, Jäger A, Kim HJ, Korn T, Kolls JK, Cantor H, Bettelli E, Kuchroo VK. Proinflammatory T helper type 17 cells are effective B-cell helpers. Proc Natl Acad Sci USA. 2010; 107:14292–14297. [PubMed: 20660725]

Pot C, Jin H, Awasthi A, Liu SM, Lai CY, Madan R, Sharpe AH, Karp CL, Miaw SC, Ho IC, Kuchroo VK. Cutting edge: IL-27 induces the transcription factor c-Maf, cytokine IL-21, and the costimulatory receptor ICOS that coordinately act together to promote differentiation of IL-10-producing Tr1 cells. J Immunol. 2009; 183:797–801. [PubMed: 19570826]

Ramirez MI, Millien G, Hinds A, Cao Y, Seldin DC, Williams MC. T1alpha, a lung type I cell differentiation gene, is required for normal lung cell proliferation and alveolus formation at birth. Dev Biol. 2003; 256:61–72. [PubMed: 12654292]

Roozendaal R, Mempel TR, Pitcher LA, Gonzalez SF, Verschoor A, Mebius RE, von Andrian UH, Carroll MC. Conduits mediate transport of low-molecular-weight antigen to lymph node follicles. Immunity. 2009; 30:264–276. [PubMed: 19185517]

Schacht V, Ramirez MI, Hong YK, Hirakawa S, Feng D, Harvey N, Williams M, Dvorak AM, Dvorak HF, Oliver G, Detmar M. T1alpha/podoplanin deficiency disrupts normal lymphatic vasculature formation and causes lymphedema. EMBO J. 2003; 22:3546–3556. [PubMed: 12853470]

Schacht V, Dadras SS, Johnson LA, Jackson DG, Hong YK, Detmar M. Up-regulation of the lymphatic marker podoplanin, a mucin-type transmembrane glycoprotein, in human squamous cell carcinomas and germ cell tumors. Am J Pathol. 2005; 166:913–921. [PubMed: 15743802]

Serafini B, Rosicarelli B, Magliozzi R, Stigliano E, Aloisi F. Detection of ectopic B-cell follicles with germinal centers in the meninges of patients with secondary progressive multiple sclerosis. Brain Pathol. 2004; 14:164–174. [PubMed: 15193029]

Spolski R, Leonard WJ. Interleukin-21: basic biology and implications for cancer and autoimmunity. Annu Rev Immunol. 2008; 26:57–79. [PubMed: 17953510]

Stromnes IM, Cerretti LM, Liggitt D, Harris RA, Goverman JM. Differential regulation of central nervous system autoimmunity by T(H)1 and T(H)17 cells. Nat Med. 2008; 14:337–342. [PubMed: 18278054]

Suzuki-Inoue K, Fuller GL, García A, Eble JA, Pöhlmann S, Inoue O, Gartner TK, Hughan SC, Pearce AC, Laing GD, et al. A novel Syk-dependent mechanism of platelet activation by the C-type lectin receptor CLEC-2. Blood. 2006; 107:542–549. [PubMed: 16174766]

Suzuki-Inoue K, Kato Y, Inoue O, Kaneko MK, Mishima K, Yatomi Y, Yamazaki Y, Narimatsu H, Ozaki Y. Involvement of the snake toxin receptor CLEC-2, in podoplanin-mediated platelet activation, by cancer cells. J Biol Chem. 2007; 282:25993–26001. [PubMed: 17616532]

Uhrin P, Zaujec J, Breuss JM, Olcaydu D, Chrenek P, Stockinger H, Fuertbauer E, Moser M, Haiko P, Fässler R, et al. Novel function for blood platelets and podoplanin in developmental separation of blood and lymphatic circulation. Blood. 2010; 115:3997–4005. [PubMed: 20110424]

Vogelzang A, McGuire HM, Yu D, Sprent J, Mackay CR, King C. A fundamental role for interleukin-21 in the generation of T follicular helper cells. Immunity. 2008; 29:127–137. [PubMed: 18602282]

Weyand CM, Kurtin PJ, Goronzy JJ. Ectopic lymphoid organogenesis: a fast track for autoimmunity. Am J Pathol. 2001; 159:787–793. [PubMed: 11549568]

Ye P, Rodriguez FH, Kanaly S, Stocking KL, Schurr J, Schwarzenberger P, Oliver P, Huang W, Zhang P, Zhang J, et al. Requirement of interleukin 17 receptor signaling for lung CXC chemokine and granulocyte colony-stimulating factor expression, neutrophil recruitment, and host defense. J Exp Med. 2001; 194:519–527. [PubMed: 11514607]

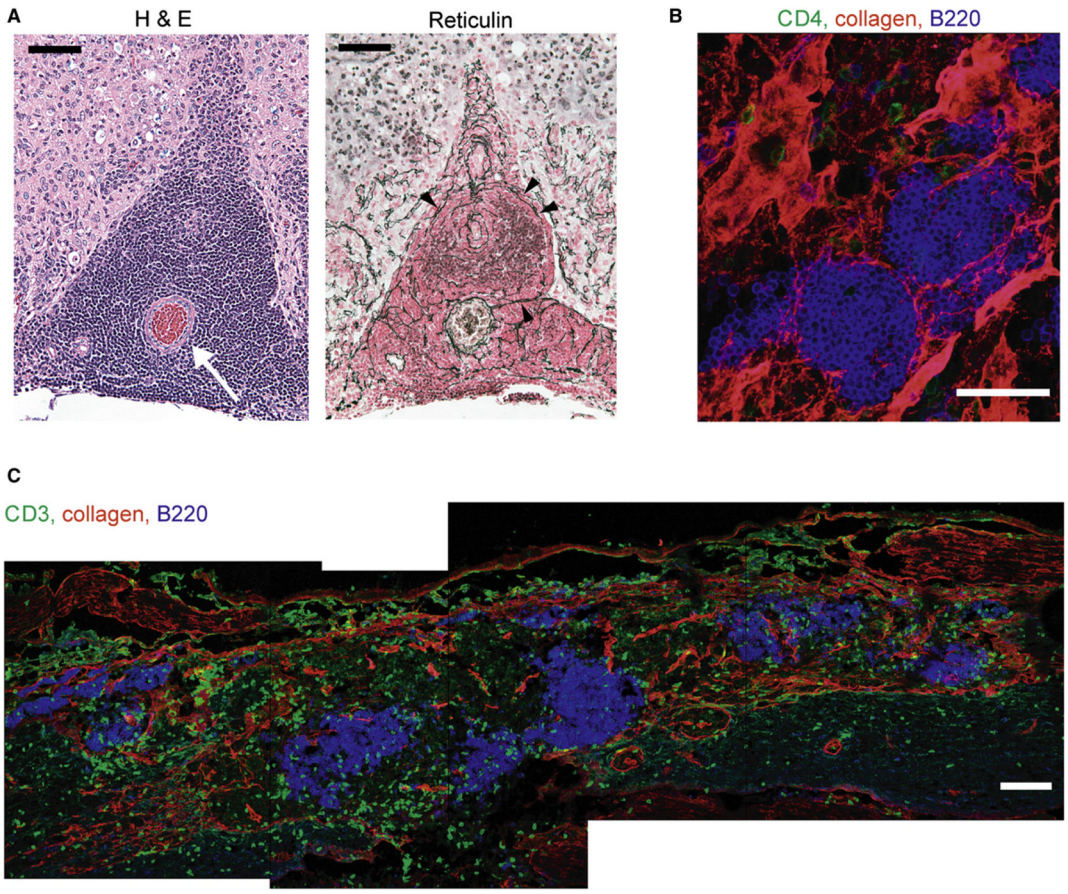

Figure 1. Recipients of MOG-Specific Th17 Cells Develop Ectopic Lymphoid Follicle-like Structures in the CNS

(A) Hematoxylin and eosin staining of a paraffin section of the anterior spinal cord of a Th17 cell recipient shows the anterior spinal columns (left and right upper corners of the field) with large aggregates of dark-blue lymphocytes within the subarachnoid space surrounding the anterior spinal artery (arrow) (left). Silver stain for reticulin reveals dark brown fibers indicating structural organization of the follicle (right, arrowheads). Note that the concentric pattern of reticulin surrounding the artery in the subarachnoid space differs from the smaller branching pattern of capillaries in the parenchyma.

(B) Cryosection of the CNS stained for B cells (B220, blue), T cells (CD4, green), and collagen (red). Scale bars represent 50 μm.

(C) Staining for T cells (CD3, green), B cells (B220, blue), and collagen (red) shows several large B cell clusters surrounded by T cells and collagen-positive fibers in the subarachnoid space. Scale bar represents 100 μm.

All pictures are representative of three or more independent experiments.

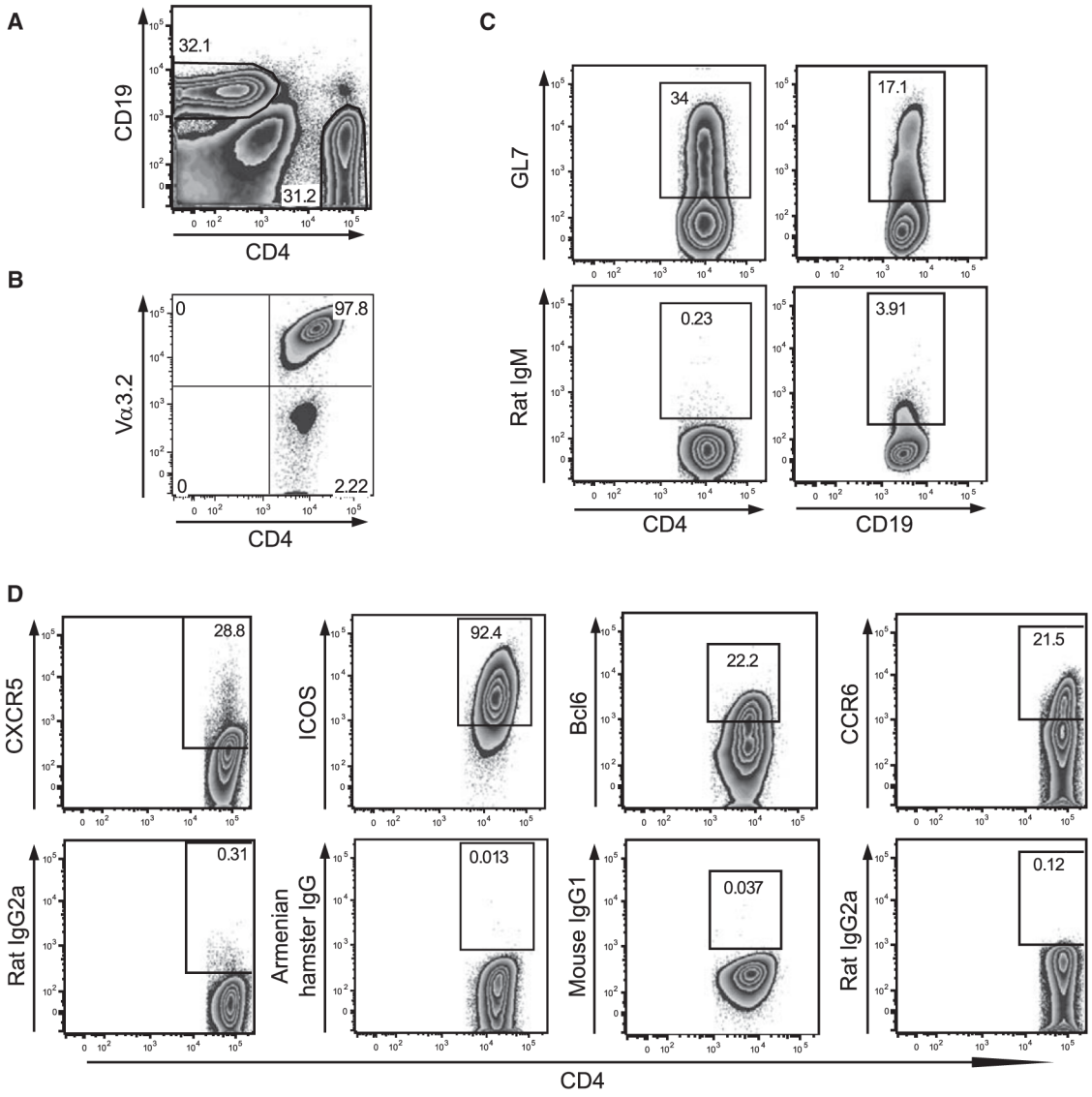

Figure 2. Th17 Cells Develop a Tfh Cell-like Phenotype in the CNS

Infiltrating cells were isolated from the CNS of Th17 cell recipients at the peak of disease, i.e., mice had a score of 2.5–4 for 3–7 days. Cells were directly stained and analyzed by flow cytometry.

(A) The infiltrating cells were tested for CD4 and CD19 expression. About 30% of the infiltrating cells were T cells (range 28%–53%) and about 30% were B cells (range 5%–32%).

(B) The infiltrating cells were tested for expression of Vα3.2, which is part of the transgenic TCR expressed on transferred T cells. The vast majority of $CD4^+$ T cells infiltrating the CNS of Th17 cell recipients are transferred cells expressing Vα3.2 (range 80%–99%).

(C) CNS T cells (left) and B cells (right) were analyzed for expression of GL7 by flow cytometry (range 15%–36% for T cells, 9%–17% for B cells).

(D) CNS-infiltrating T cells were analyzed for expression of CXCR5 (range 9%–90%), ICOS (range 40%–95%), Bcl6 (range 13%–27%), and CCR6 (range 5%–31%) by flow cytometry.

Flow cytometry data shown are representative of at least six individual mice from two or three independent in vivo experiments.

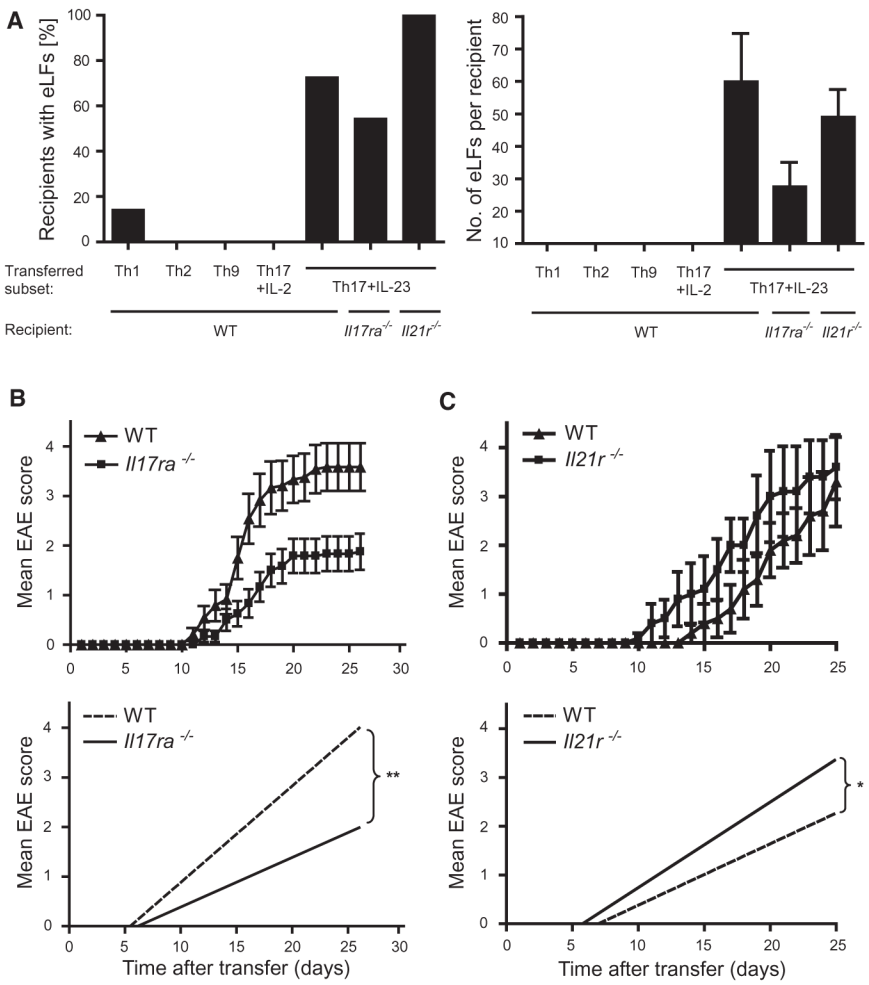

Figure 3. Formation of Ectopic Lymphoid Follicle-like Structures in the CNS Depends Partly on IL-17 but Not IL-21

(A) WT, *Il17ra*$^{-/-}$, and *Il21r*$^{-/-}$ recipients of different MOG-specific T cell subsets were monitored for disease development. 30–40 days after transfer, the CNS of the recipients was harvested and analyzed for the incidence (left) and number (right) of eLFs. Only recipients that developed disease and survived are represented in the graphs. For the quantification (right), only mice with ten or more eLFs in the CNS were considered positive and included in the analysis. Error bars represent SEM. Graphs show combined data from two to four independent in vivo experiments per column.

(B and C) Th17 cells were adoptively transferred into WT and *Il17ra*$^{-/-}$ recipients (B) or into WT and *Il21r*$^{-/-}$ recipients (C) and mice were monitored for the development of disease. Whether disease courses were significantly different between the groups was analyzed by linear regression analysis (B, bottom, **$p < 0.0001$, and C, bottom, *$p < 0.01$). Graphs in (B) show combined data from two independent experiments (three independent experiments were performed), and graphs in (C) are representative of three independent experiments.

Error bars represent SEM. Further information can be found in Table S1.

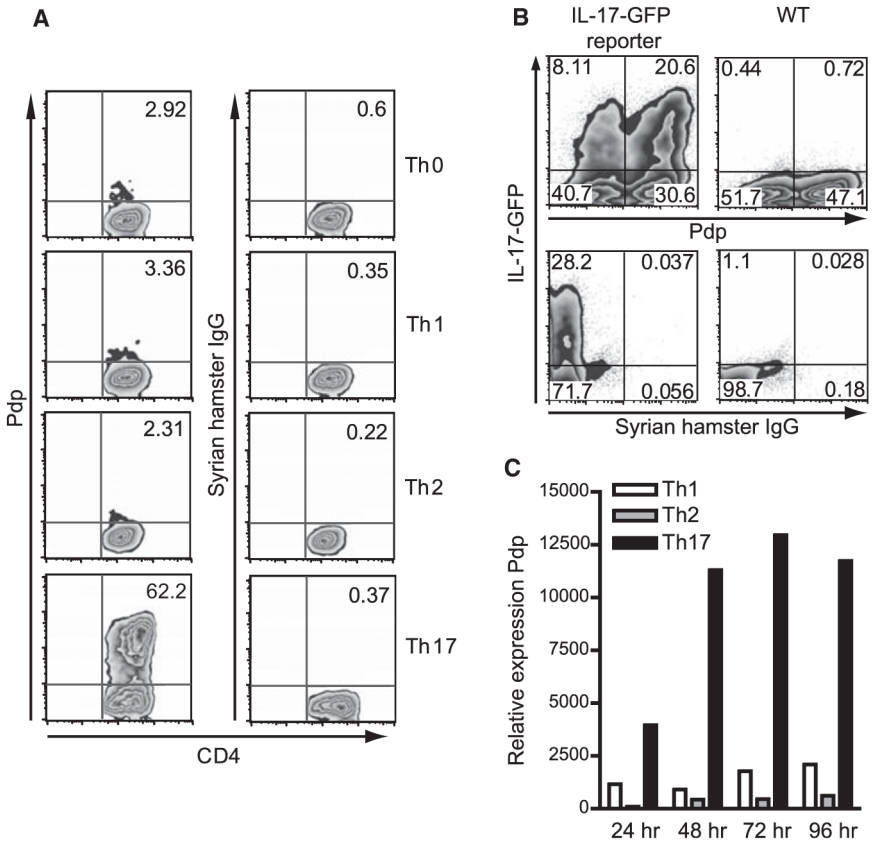

Figure 4. Podoplanin Is Specifically Expressed on Th17 Cells In Vitro

(A) Sorted naive $CD4^+$ T cells were differentiated in vitro into different T cells subsets, and after 4 days expression of Pdp was determined by flow cytometry.

(B) Sorted naive T cells from WT or IL-17-GFP reporter mice were differentiated in vitro with IL-6+TGF-β. After 4 days, expression of Pdp and IL-17-GFP was analyzed by flow cytometry.

(C) After restimulation of in-vitro-differentiated Th1, Th2, and Th17 cells with anti-CD3 and anti-CD28, mRNA levels of Pdp were measured at the indicated time points.

Data shown are representative of at least three independent experiments.

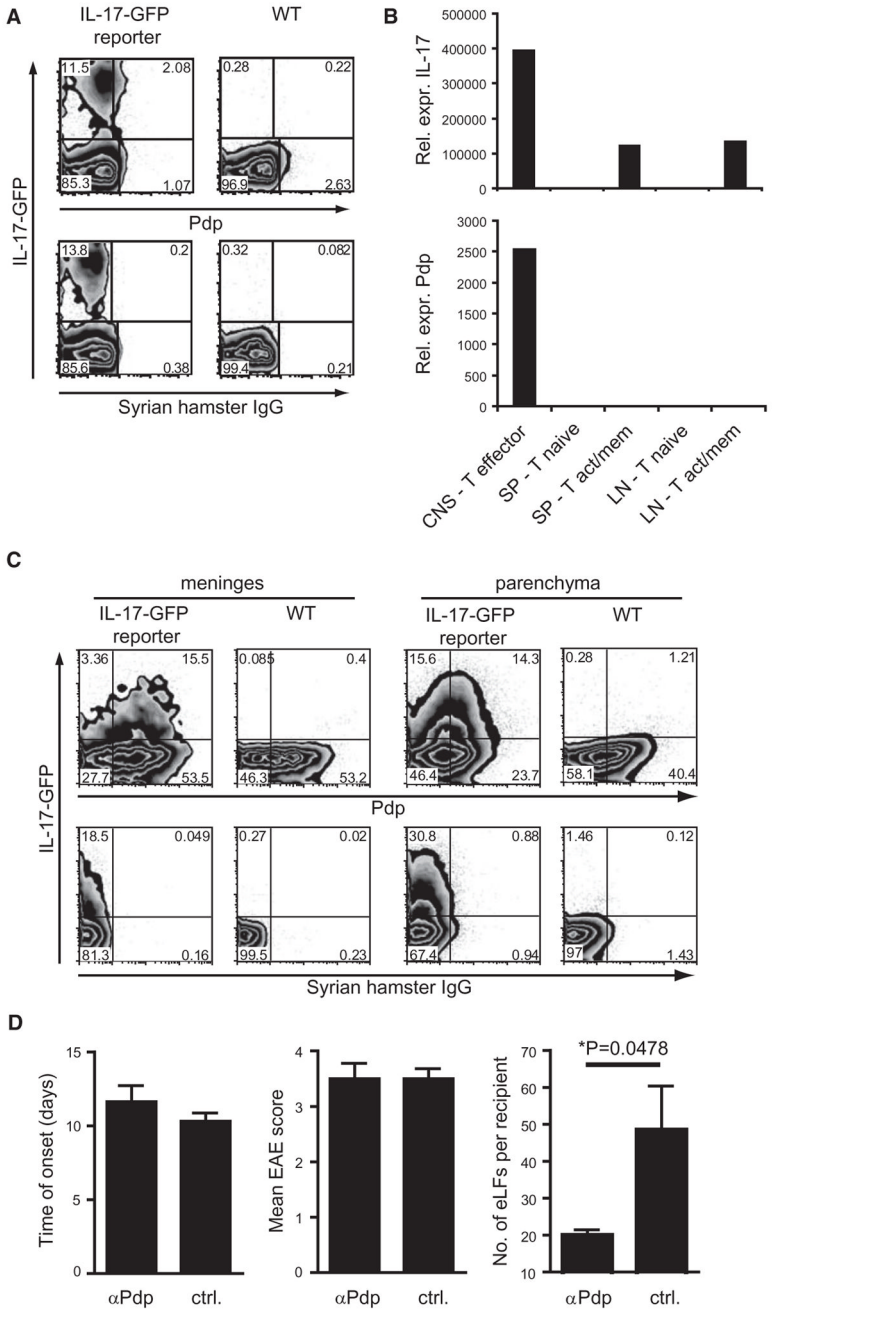

Figure 5. Pdp Is Expressed on Th17 Cells In Vivo and Is Important for Formation of the Ectopic Lymphoid Follicle-like Structures in Th17 Cell Recipients

(A–C) WT and IL-17-GFP reporter mice were immunized with 100 μg MOG in CFA. (A) On day 8 after immunization, splenocytes were harvested and cultured in the presence of MOG. After 4 days T cells were stimulated with PMA and ionomycin in the presence of monensin for 4 hr and analyzed for expression of IL-17-GFP and Pdp by flow cytometry. Data shown are representative of nine mice per group from two independent in vivo experiments.

(B) At the peak of disease, T cells were sorted from the CNS, spleen, and LNs and mRNA levels of IL-17 and Pdp were determined by quantitative PCR. Graphs are representative of two independent in vivo experiments.
(C) At the onset of disease, infiltrating cells were isolated from meninges and CNS parenchyma and expression of Pdp and IL-17-GFP on $CD4^+$ T cells was determined by flow cytometry directly ex vivo. Data shown are representative of four mice per group from two independent experiments.
(D) Th17+IL-23 cells were transferred into WT recipients treated with 100 μg polyclonal anti-Pdp on day 0, 2, 4, and 7 after transfer. Control animals were treated with goat IgG or PBS. Mice were monitored daily for development of EAE, and 30–40 days after transfer, the CNS of recipients was harvested for histological analysis. Bar graphs show the time of disease onset (left), the mean maximum disease score (middle), and the number of eLFs per recipient (right) for the anti-Pdp-treated mice versus control mice. Graphs show combined data from two independent experiments. Error bars represent SEM. The difference between the groups was tested for significance by an unpaired Student's t test with Welch's correction (*p = 0.0478) (right). Further information can be found in Table S2.

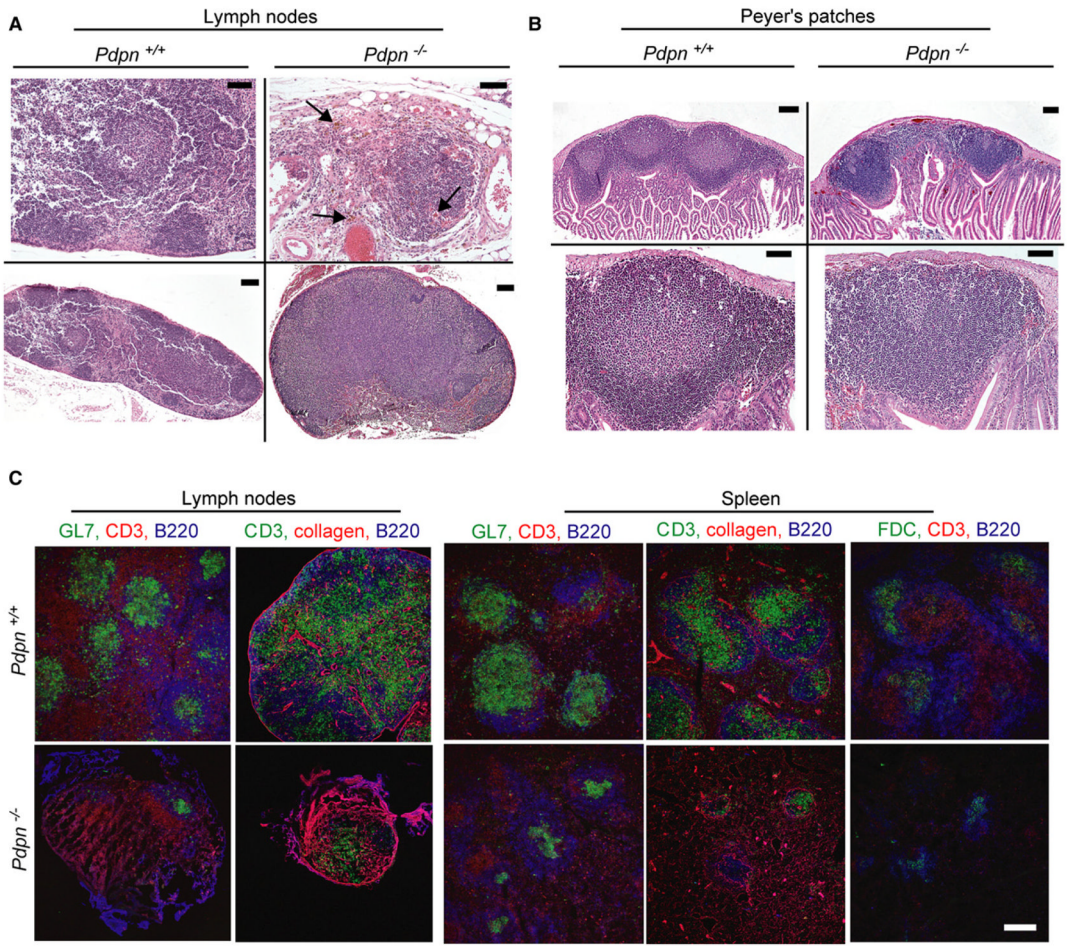

Figure 6. Pdp-Deficient Mice Have a Defect in the Formation of Secondary Lymphoid Structures

(A) Hematoxylin and eosin staining of paraffin sections of a LN harvested from a *Pdpn*$^{+/+}$ mouse (left), a LN remnant harvested from a *Pdpn*$^{-/-}$ mouse (top right), and a rare normal-sized LN harvested from a *Pdpn*$^{-/-}$ mouse (bottom right). Lymphocytes stain dark blue and extravasated red blood cells stain red (arrows, top right).

(B) Hematoxylin and eosin staining of a paraffin section of PP harvested from *Pdpn*$^{+/+}$ mice (left) and *Pdpn*$^{-/-}$ mice (right). Top panels show whole PP, and bottom panels show one follicle of the PP.

(C) Cryosections from LNs, LN remnants, and spleens of 12-month-old *Pdpn*$^{-/-}$ mice and their *Pdpn*$^{+/+}$ littermates were analyzed for GC structure via T cell-specific (CD3), B cell-specific (B220), and FDC-specific stains (αCR1, clone 8C12), as well as the GC marker GL7 and the structural marker collagen.

Data shown are representative of three independent experiments. Scale bars in (A) (top) and (B) (bottom) represent 50 μm. Scale bars in (A) (bottom) and (B) (top) represent 100 μm. Scale bar in (C) represents 200 μm.